New Oxidation Pathway of 3,5-Di-*tert*-butyl-4-hydroxytoluene: An Ionspray Tandem Mass Spectrometric and Gas Chromatographic/Mass Spectrometric Study

Nan Zhang*, Shoji Kawakami, Masato Higaki, and Victorio T. Wee

Procter & Gamble Asia, Kobe Technical Center, Kobe 658, Japan

ABSTRACT: The autoxidation of 3,5-di-*tert*-butyl-4-hydroxytoluene (BHT, **1**) in bar soap was investigated with ionspray tandem mass spectrometric and on-line gas chromatographic/mass spectrometric methods. The oxidation products of BHT were extracted from the bar soap surface, concentrated, and fractionated with open-column chromatography to remove the impurities. New oxidation products of BHT (BHT phenol-type dimer **7** and others) were identified with the two mass spectrometric methods. The results suggested that oxidation of BHT in bar soap occurred in a way different from that in the previous studies. In the new pathway, oxidation of BHT first generates an excited state of phenol-type dimer **4**, and then this species decomposes, due to its high energy, to form dimer **7**. The mechanism of oxidation is discussed.

JAOCS 74, 781–786 (1997).

KEY WORDS: Autoxidation, 3,5-di-*tert*-butyl-4-hydroxytoluene, gas chromatography, mass spectrometry, reaction mechanism.

Autoxidation of consumer products is one of the most common problems that many manufacturers face. The oxidation of consumer products due to aging, and more specifically, due to reactions initiated by heat, light and molecular oxygen, usually leads to color changes of the consumer products. To prevent autoxidation, antioxidants are added into the consumer products. 3,5-Di-*tert*-butyl-4-hydroxytoluene (BHT, **1**, Scheme 1), which is widely used in the food and consumer product industry, is one such antioxidant, which can be added intentionally, or exists in some raw materials from natural sources.

BHT itself can be oxidized to yellowing dimers (both phenol and quinone types) and has been studied before (1–11). The structures, the main reported oxidation dimers, and the oxidation mechanism of BHT (1–11) are summarized in Scheme 1. It is generally accepted that the oxidation of BHT starts with the hydrogen abstraction reaction of organic peroxy radicals (ROO·), and then the BHT radicals (**2** and **3**, Scheme 1) formed recombine to form phenol-type BHT dimers (**4** and **5**, Scheme 1). The phenol-type BHT dimers can be further oxidized to their quinone-type dimer (**6**, Scheme 1), which has a characteristic yellow color. These yellowing dimers may cause problems for many types of consumer products. The oxidation of BHT studied so far has been

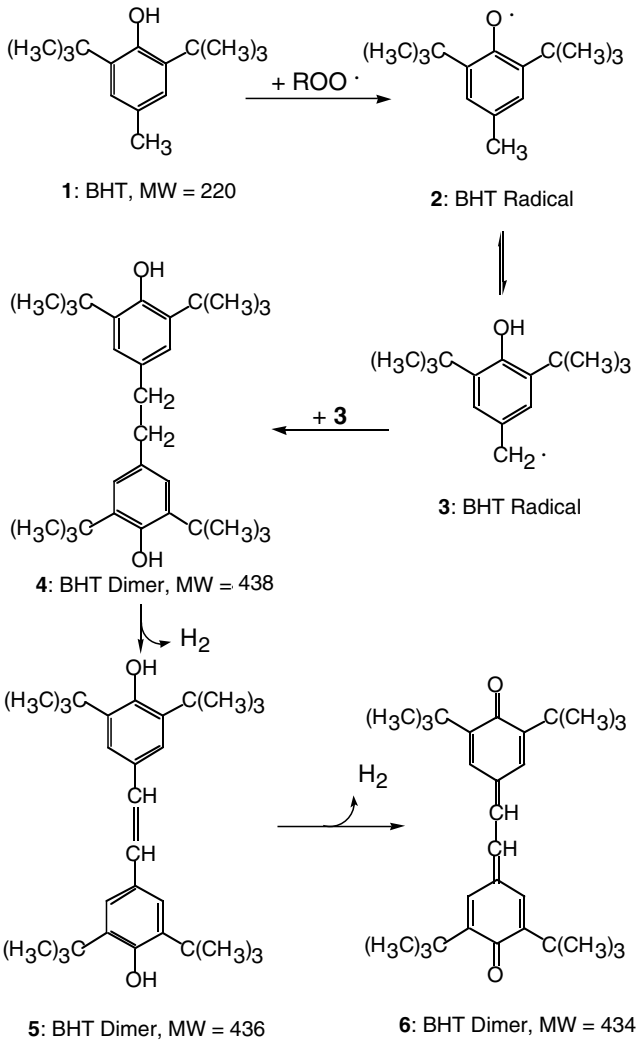

SCHEME 1

*To whom correspondence should be addressed at Procter & Gamble Asia, Kobe Technical Center, 17, Koyo-cho Naka 1-chome, Higashinada-ku, Kobe 658, Japan. E-mail: zhangn@pg.com.

performed, in most cases, in solution and under quite intensive oxidation conditions, such as low-valence transition metal salts (5) or ultraviolet radiation (9), and in rubber-base materials (10).

Mass spectrometry (MS) has found widespread use in oxidation studies of pharmaceutical chemicals (12–14) due to its ability to provide unambiguous determination of analyte structure. The recently developed ionization techniques, electrospray (ESI) and atmospheric pressure chemical ionization (APCI), have been successfully used in analyses of nonvolatile drug-related compounds (15–17). Ionization by ESI and APCI is soft and produces predominantly molecular species *via* proton or sodium transfer reactions. Collison-induced dissociation (CID) can be used to obtain a sufficient number of characteristic fragment ions for structure elucidation of unknowns.

In the present study, it was our goal to develop a quick mass-spectrometric (MS) method to monitor the oxidation of BHT in bar soap. The BHT oxidation products were extracted from yellowed soap, concentrated, fractionated with open column chromatography, and identified with MS. We will report new oxidation products and new oxidation mechanism of BHT in bar soap.

EXPERIMENTAL PROCEDURES

Reagents and supplies. High-performance liquid chromatography (HPLC)-grade methanol (99.7%), hexane (96.0%), and acetonitrile (99.8%) were obtained from Kanto Chemical Co., Inc. (Tokyo, Japan). Trifluoroacetic acid (TFA, 98.0%) was obtained from Wako Pure Chemical Industries Ltd. (Osaka, Japan). The calibration reagent for ionspray (IS)/MS, poly(propylene glycol) (PPG), was obtained from the Sciex API III supplier (Ontario, Canada). It contained 3.3×10^{-5} M of PPG 425, 1×10^{-4} M of PPG 1000, 2×10^{-4} M of PPG 2000, 2×10^{-3} M of ammonium acetate, 0.1% acetonitrile and 0.1% formic acid dissolved in a 50:50 solution of water/methanol. HPLC-grade water was used in all studies.

Bar-soap aging procedure and sample preparation. The bar soaps, which contained BHT, were kept under normal storage conditions for 3 mon. The soaps were packaged with a stiffener and a wrapper, and stored in a warehouse at room temperature and common humidity. Part of the soap surface turned to a bright yellow color. The yellow part of the soap surface (the first thin layer) was collected and then extracted with methanol. The methanol solution was concentrated to remove part of the soap, which precipitated during the concentration. The methanol was completely evaporated to collect the yellow residue. The yellowing materials were extracted from the residue with acetonitrile to remove more soap. After concentration of the acetonitrile extract to near dryness, the residue was subjected to column chromatography [silica gel C-200 with ethyl acetate:hexane (1:9, vol/vol) as mobile phase] to yield two main fractions for MS analysis. The first fraction was not yellow while the second was yellow. Both yellowing and nonyellowing samples were diluted to a proper concentration with methanol to give ion intensities of around 1×10^6 counts/s in the IS/MS spectra. TFA (0.02%) was added to the samples as ionization agent for the positive ion mode analysis, and 0.2% ammonia for the negative ion mode analysis.

MS. The appropriately diluted samples in methanol were first subjected to IS/MS and IS/MS/MS analyses, which was performed on a Sciex API-III (SCIEX Inc) MS with an ionspray interface (pneumatically assisted electrospray). The API-III, both Q1 and Q3, was tuned and calibrated every day with the PPG calibration reagent with a mass accuracy of $\Delta m \leq 0.1$ over the mass range *m/z* 50–2200. Both mass analyzers were operated at unit mass resolution.

Both Q1 and Q3 mass spectrometers of the Sciex API-III were run at both positive and negative ion modes. The following conditions (positive and negative ion mode, respectively) were used for sample analyses: IS interface tip voltage (ISV on Sciex), +5000 V and −4500 V with respect to the ion entrance of the mass spectrometer; orifice voltages for both MS and MS/MS experiments, or the declustering energies being the potential difference between the orifice and the AC rods, were +60 V and −60 V; nebulizer gas pressure, 40 psi (air, 0.6 L/min); curtain gas flow rate, 0.6 mL/min (ultra-high purity nitrogen, 99.999%). The orifice temperature was kept at 45°C. The Sciex instrument uses an open-rod collison cell configuration for CID in the MS/MS analyses. Ultra-pure argon (99.999%) was used as collision gas, which was measured as collision gas thickness (CGT). The CGT for this experiment was 300×10^{12} molecules/cm^2. The collision energies were optimized for each target compound.

The mass spectra were normally obtained with an averaging of 10 scans. The mass spectrometer was scanned from *m/z* 150 to 600 to cover all possible ions in the IS/MS experiments. A 1-millisecond dwell time for each scan was used. For IS/MS/MS experiments, the parent ion was selected by the first quadrupole analyzer, subjected to CID in the second quadrupole, and then the third quadrupole analyzer was scanned from *m/z* 10 to the mass number 10 or 20 units higher than that of the parent ions.

Secondly, the samples were subjected to GC/MS analysis for further structural confirmation in a Shimadzu GC-14A, coupled with a Profile HV-400 mass spectrometer from Kratos (Ramsey, NJ). The GC conditions were: capillary column DB-5, 30 m × 0.25 mm (i.d.) with splitless injection; stationary phase, 5% diphenyl and 95% dimethyl polysiloxane; film thickness, 0.25 μm; programmed oven temperature from 45 to 320°C at a rate of 10°C/min. The GC/MS experiments were conducted at a scan speed of 0.4 s per decade with both EI (70 eV of electron beam energy) and CI (isobutane reagent gas, 150 eV of electron beam energy) ionization techniques.

RESULTS AND DISCUSSION

IS/MS/MS study. Both yellowing and nonyellowing samples were first subjected to IS/MS analysis under positive ion

mode. The MS spectra showed that there were many components in both samples. To determine the difference between the two samples, a technique called spectral subtraction was used, in which the spectrum of the nonyellowing sample was subtracted from that of the yellowing sample. The new spectrum, which should contain the information about the yellowing materials, is shown in Figure 1. The most interesting mass peaks were *m/z* 383, 405, 327, 271, 279, 301.

The mass numbers *m/z* 383 and 405 were consistent with the proton and sodium adducts ([M + H^+] and [M + Na^+], respectively) of BHT phenol-type dimer **7**: 1-(3,5-di-*tert*-butyl-4-hydroxyphenyl)-2-(3′-*tert*-butyl-4′-hydroxyphenyl)-ethane (see structure in Scheme 2). To prove this assignment, a MS/MS study was performed. The result is shown in the inset in Figure 1. It clearly shows that the CID of the proton adduct of BHT dimer **7** could generate fragment ions with *m/z* 327, 271, 239, and 57. The fragmentation reaction pathways are proposed as in Scheme 2. The ion *m/z* 327 was formed *via* a rearrangement of a hydrogen atom and loss of *tert*-butylene [CH_2=$C(CH_3)_2$] from the parent ion due to protonation at the benzene ring. Following the same procedure, the ion *m/z* 327 was further fragmented into ion *m/z* 271 by losing one other molecule of butylene. Ion *m/z* 239 might be formed from ion *m/z* 271 by loss of first CH_2O and then H_2 after extensive hydrogen and carbon rearrangements. The ion *m/z* 239 may have a structure of *tert*-butylphenol tropylium ion. This ion relationship (from *m/z* 271 to 239) was supported by the fact that ion *m/z* 239 was the main fragment ion in a "pseudo" MS/MS/MS experiment on fragment ion *m/z* 271. In this experiment, the ion *m/z* 271 was first produced in the IS and then mass-selected for further MS/MS. The ion *m/z* 57 was consistent with ion $(CH_3)_3C^+$, which was formed due to an inductive cleavage of the parent ion. All these characteristic fragment ions support the above structural assignment.

The mass numbers *m/z* 327 and 271 in the IS/MS spectrum were identified as fragment ions of BHT dimer **7** due to the ionization process. The intensities of these ions can be reduced by decreasing the orifice voltage since a lower orifice voltage would induce less fragmentations. This was also supported by the fact that there were no sodium adducts of these ions observed in the IS/MS spectrum.

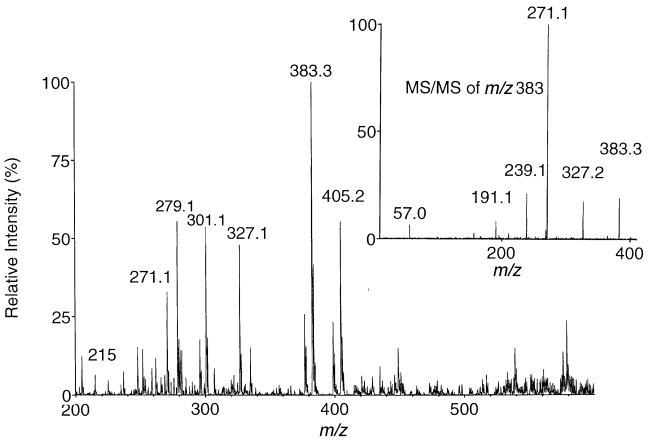

FIG. 1. The IS/MS spectrum of the oxidation products of BHT under the positive ion mode. Inset: The IS/MS/MS spectrum of BHT dimer **7**.

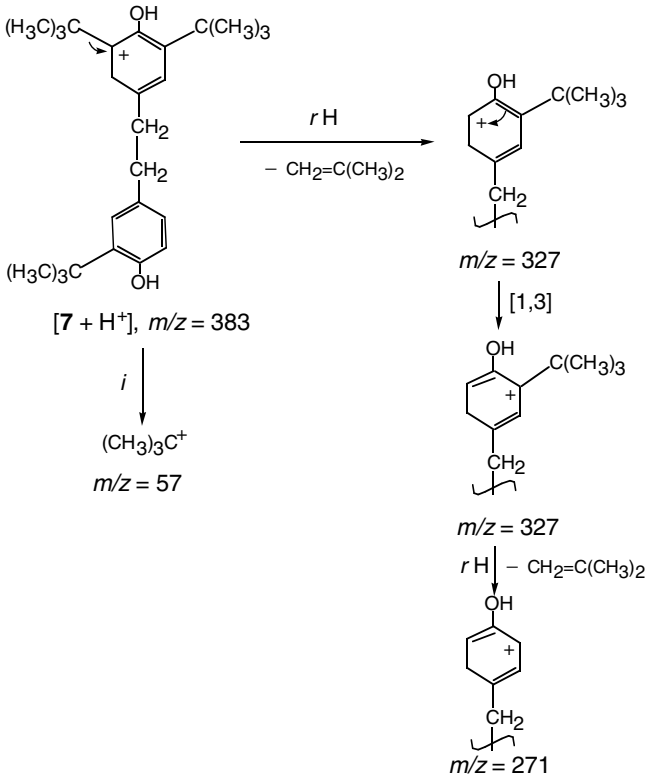

SCHEME 2

Observation of the sodium adduct of dimer **7** suggests that this component existed in the sample prior to ionization, and thus, it was not the fragment ion from dimer **4** because sodium adducts are usually stable in the IS. This point is further supported by the fact that, even with the lowest orifice voltage of 35 V, the minimal fragmentation due to orifice collision, the ion corresponding to **4** was not observed. The mass numbers *m/z* 279 and *m/z* 301 were identified, based on the MS/MS spectra (not shown), as proton and sodium adducts of an uncharacterized compound [**3** + R], in which R is most likely C_3H_7O.

To confirm the presence and structure of **7** in the sample, the yellowing sample was subjected to IS/MS and MS/MS analysis under the negative ion mode. The IS/MS spectrum is shown in Figure 2. The ion corresponding to phenoxide ion of **7** with *m/z* 381 ([M − H]$^-$) was observed. The MS/MS spectrum is shown in the inset in Figure 2. The phenoxide ion of **7** (CID energy: 25 eV in laboratory frame) is much more stable in the CID study than the proton adduct of **7** (CID energy: 15 eV in laboratory frame). The results in Figure 2 indicate that the phenoxide ion of **7** could lose two $CH_3^{\cdot}$ radicals sequentially to produce fragment ions *m/z* 366 and 352, as well as butylene to produce ion *m/z* 325.

GC/MS study. Both yellow and nonyellow samples were also subjected to GC/MS analysis with EI and CI ionization

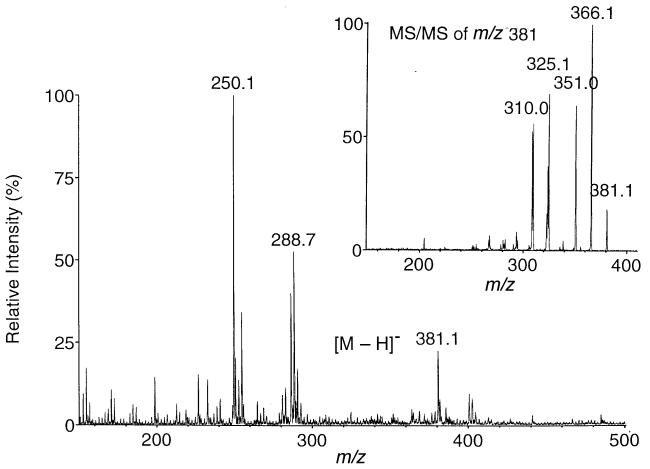

FIG. 2. The IS/MS spectrum of the oxidation products of BHT under the negative ion mode. Inset: The IS/MS/MS spectrum of the phenoxide ion of BHT dimer **7**.

modes, respectively. The GC/EI–MS and GC/CI–MS spectra of compound **7** are shown in Figure 3A and B. The parent ions with *m/z* 382 for $M^{+\cdot}$ and *m/z* 383 for $[M + H^+]$ of BHT dimer **7** were observed in EI and CI mode, respectively. Again, the fragmentation patterns in both mass spectra confirmed the structure of **7**. As shown in Figure 3, the EI spectrum gave fragment ions with *m/z* 367, 326, 311, 269, and 57 (not shown in the figure), while the CI spectrum gave fragment ions with *m/z* 327 and *m/z* 271 which were similar to those of the IS/MS/MS experiment. We noticed that, in the CI spectrum, the odd-electron parent ion *m/z* = 382 ($OE^{+\cdot}$) and some of its fragment ions also existed. In the EI spectrum, all important fragment ions can be reasonably explained by the reactions shown in Scheme 3. Ionization at the hydroxy group will lead to a [1,5] hydrogen rearrangement [McLafferty rearrangement (18)] to produce a BHT methyl radical that can

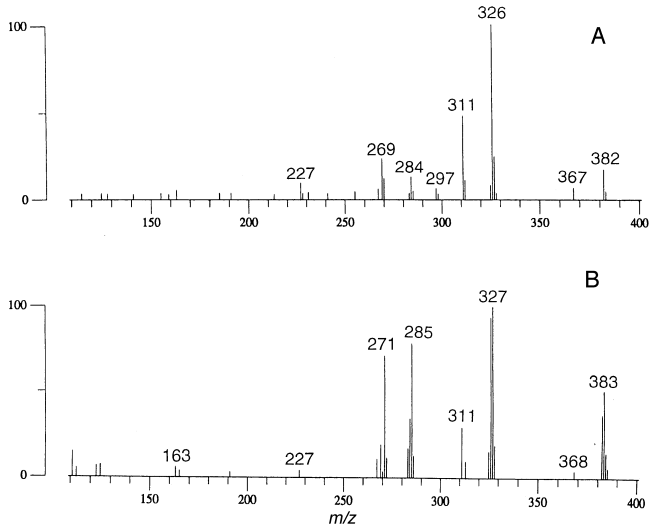

FIG. 3. The GC/MS spectra of BHT dimer **7** under (A) EI and (B) CI modes.

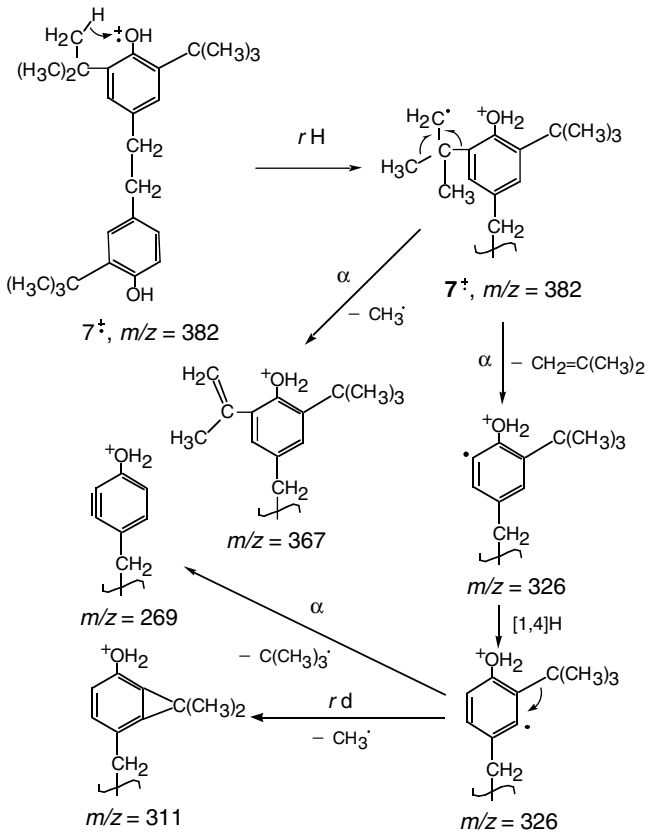

SCHEME 3

initiate two parallel α cleavages to generate ions *m/z* 367 and 326. Starting from the ion *m/z* 326, ions *m/z* 269 and *m/z* 311 can be formed *via,* respectively, an α cleavage and *rd* rearrangement after a [1,4] hydrogen rearrangement at the benzene ring. Ion *m/z* 57 could be formed *via* an inductive cleavage when the ionization occurred at the benzene ring. We also found in the GC/MS study that compound **7** is the only BHT-related oxidation dimer in the yellowing sample.

Oxidation mechanism. Many factors can initiate the oxidation of BHT. Heat or light can induce free-radical formation in many organic systems (19). The oxidation of BHT can be initiated by the hydrogen abstraction of peroxy radical ROO·. This free radical initiated a multiple-step reaction that led to the formation of the dimers of BHT. Briefly, the oxidation reactions can be described by the reaction pathways in Scheme 4.

It is easy to imagine that the recombination of radical **3** will produce **4**. This is true for most studies (in solution) in the literature (2,3,5). However, this reaction is not necessarily true under some other reaction conditions, for example, the reaction in solid state (like in soap). A more complete BHT oxidation mechanism is proposed: The recombination of radical **3** produces an excited state of **4** (**4***) before the bond energy [referring to the bond energy of $C_6H_5CH_2$–CH_3 which is about 79 kcal/mol (≈3.4 eV) (20)] released due to a new C–C bond formation is removed. In solution, this excited state can be quickly quenched by solvent-molecule collision (to re-

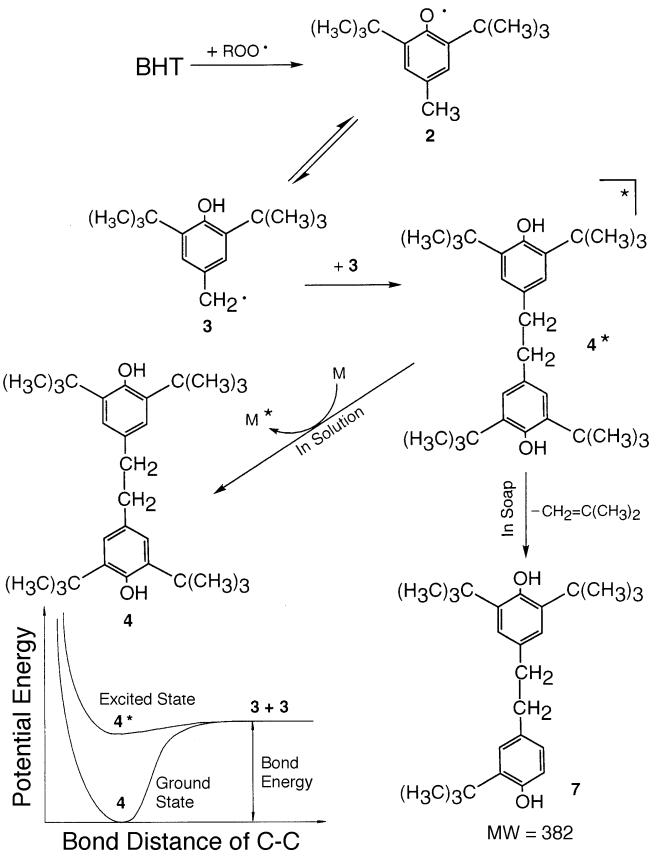

SCHEME 4

move the extra energy deposited into the molecules), thus producing **4**. However, in soap, because of insufficient solvent molecule collision where the molecules in soap are not as free as those in solution, this extra energy is used to cleave one molecule of butylene from **4*** to produce **7**.

The potential energy curve that describes this reaction system is also illustrated in the inset of Scheme 4. When two BHT radicals (**3**) come close to each other, the distance between the two carbon atoms, which have one free electron each, gets smaller and smaller, leading to formation of a C–C bond. When the new C–C bond is formed and the bond energy is dissipated, the stable ground state of **4** is formed. If there is no efficient way to remove the bond energy, the excited state (**4***) of **4** will be formed. This species is unstable and will decompose to dimer **7**. This proposed pathway is quite similar to the CID in the IS/MS/MS study, in which the proton adduct of **7** is activated *via* energetic collision (25 eV at lab frame ≈2.4 eV at center-of-mass frame) with argon atoms. Part of the collision energy was deposited into the molecule and causes decomposition to small fragments by loss of butylene.

In conclusion, during the study of the oxidation of BHT in bar soap with IS/MS/MS and GC/MS techniques, new oxidation products (dimer **7** and others) were identified. The observation of compound **7** suggests a new oxidation mechanism, which led us to modify the present oxidation mechanism of BHT to a more complete one. In the new mechanism, oxidation of BHT first generates an exicted state (**4***) of the phenol-type dimer **4**, and then this species decomposes to dimer **7**.

ACKNOWLEDGMENTS

The authors thank C. Salvador and X.C. Hu for their fruitful discussions.

REFERENCES

1. Squirrel, D.C.M., Analysis of Additives and Process Residues in Plastics Materials, *Analyst 106*:1042–1056 (1981).
2. Folley, L., and F.M. Kimmerle, Pulse Voltammetric Determination of Butylated Hydroxy Toluene in Transformer Oils, *Anal. Chem. 51*:818–822 (1979).
3. Bromberg, A., and K.A. Muszkat, Oxidation of 4a,4b-Dihydrophenanthrenes. I. Kinetics of the Thermal Reaction of 9,10-Cyclopentano-4a,4b-dihydrophenanthrene with Oxygen, *J. Am. Chem. Soc. 91*:2860–2866 (1969).
4. Thompson, D.C., Y.N. Cha, and M.A. Trush, The Peroxidase-Dependent Activation of Butylated Hydroxyanisole and Butylated Hydroxytoluene (BHT) to Reactive Intermediates, *J. Biol. Chem. 264*:3957–3965 (1989).
5. Maumy, M., and P. Capdevielle, Chemical Evidence for Peroxy Radicals Intermediacy in Copper (II) Reaction with Hydroperoxides, *Tetrahedron 19*:7455–7462 (1993).
6. Pokorny, J., *Autoxidation of Unsaturated Lipids,* edited by H.W.-S. Chan, Academic Press Inc. (London) Ltd., 1987, p. 169.
7. Bolton, J.L., Oxidation of Butylated Hydroxytoluene to Toxic Metabolites, *Drug Metab. Dispos. 19*:467–472 (1991).
8. Bolton, J.L., Formation and Reactivity of Alternative Quinone Methides from Butylated Hydroxytoluene: Possible Explanation for Species-Specific Pneumotoxicity, *Chem. Res. Toxicol. 3*:65–70 (1990).
9. Kurechi, T., and T. Kato, Study on the Antioxidants: XI. Oxidation Products of Concomitantly Used Butylated Hydroxyanisole and Butylated Hydroxytoluene, *J. Am. Oil Chem. Soc. 57*:220–223 (1980).
10. Spitz, H.D., Determination of 2,6-Di-(*tert*-butyl)-4-methylphenol in Rubber-Base Materials and Identification of an Oxidation Product from 2,6-Di-(*tert*-butyl)-4-methylphenol, *J. Chromatogr. 190*:193–196 (1980).
11. Majcherczyk, C., P. Polge, D. Baylocq, and F. Pellerin, Action des Rayonnements beta et des Oxydants sur le Di-*tert*-butyl-3,5 hydroxy-4 toluene, *Talanta 33*:985–989 (1986).
12. Segarra, V., F. Carrera, J.L. Fabregas, and J. Claramunt, Degradation Profile and Identification of the Major Degradation Products of Dobupride Under Several Conditions by GC/MS and HPLC-Particle Beam/MS, *J. Pharm. Biomed. Anal. 13*:987–993 (1995).
13. Schiavi, M., S. Serafini, A. Italia, M. Villa, G. Fronza, and A. Selva, Identification of the Major Degradation Products of 4-Methoxy-2-(3-phenyl-2-propynyl)phenol Formed by Exposure to Air and Light, *J. Pharm. Sci. 81*:812–814 (1992).
14. Jedlitschky, G., M. Huber, A. Volkl, M. Muller, I. Leider, J. Muller, W.D. Lehmann, H.D. Fahimi, and D. Keppler, Peroxisomal Degradation of Leukotrienes by β-Oxidation from the ω-End, *J. Biol. Chem. 266*:24763–24772 (1991).
15. Poon, G.K., Y.C. Chui, G.M.F. Bisset, and M. Jarman, Analysis of Anti-Cancer Drugs by Electrospray Ionization Mass Spectrometry, *Proceedings of the Kyoto 92 International Conference on Biological Mass Spectrometry,* edited by T. Matsuo, San-ei Publishing Co., Kyoto, Japan, 1992, pp. 396–397.
16. van Breemen, R.B., C.-R. Huang, Z.Z. Lu, A. Rimando, H.H.S.

Fong, and J.F. Fitzloff, Electrospray Liquid Chromatography/Mass Spectrometry of Ginsenosides, *Anal. Chem. 67*:3985–3989 (1995).
17. Taylor, L.C.E., R. Singh, S.Y. Chang, and R.L. Johnson, The Identification of *in vitro* Metabolites of Bupropion Using Ion Trap Mass Spectrometry, *Rapid Comm. Mass Spectrom. 9*:902–910 (1995).
18. McLafferty, F.W., and F. Turecek, *Interpretation of Mass Spectra,* 4th edn., University Science Books, Sausalito, 1993, pp. 72.
19. Morrison, R.T., and R.N. Boyd, *Organic Chemistry,* 6th edn., Prentice Hall, Englewood Cliffs, 1992, p. 47.
20. Lide, D.R., *CRC Handbook of Chemistry and Physics,* 73rd edn., CRC Press, Boca Raton, 1992, pp. 9–14.

[Received November 12, 1996; accepted April 17, 1997]